JLAB USER GROUP

Jefferson Lab PAC15

Proposal Cover Sheet

This document must be received by close of business Thursday, Dec 17, 1998 at:

Jefferson Lab
User Liaison,
Mail Stop 12B
12000 Jefferson Ave.
Newport News, VA
23606

Experimental Hall: A

Days Requested for Approval: 30

❒ Proposal Title:
A Clean Measurement of the Neutron Skin of ^{208}Pb Through Parity Violating Electron Scattering

Proposal Physics Goals
Indicate any experiments that have physics goals similar to those in your propos

Approved, Conditionally Approved, and/or Deferred Experiment(s) or proposals:

Contact Person
Name: Robert Michaels
Institution: Jefferson Lab
Address: 12000 Jefferson Ave
Address:
City, State, ZIP/Country: Newport News, VA 23606 USA
Phone: (757) 269 7410 Fax: (757) 269 5235
E-Mail: rom @ jlab.org

Jefferson Lab Use On

Receipt Date: 12/17/98 PR-99-012

By: [redacted]

BEAM REQUIREMENTS LIST

JLab Proposal No.: _____ Date: Dec 16, 1998

Hall: A Anticipated Run Date: 2002 PAC Approved Days: 30

Spokesperson: Robert Michaels, & Paul Souder Hall Liaison: Robert Michaels
Phone: (757) 269 7410
E-mail: rom @ jlab.org

List all combinations of anticipated targets and beam conditions required to execute the experiment. (This list will form the primary basis for the Radiation Safety Assesment Document (RSAD) calculations that must be performed for each experiment.)

Condition No.	Beam Energy (MeV)	Mean Beam Current (μA)	Polarization and Other Special Requirements (e.g., time structure)	Target Material (use multiple rows for complex targets — e.g., w/windows)	Material Thickness (mg/cm²)	Est. Beam-On Time for Cond. No. (hours)
1.	850	50	strained GaAs	^{208}Pb	635	690 *
			with maximum	^{9}Be	9	690 *
			polarization (~80%)			
2	850	0.005	same	^{208}Pb	20	20
		(0.5 μA		(or ^{12}C)		
		pulsed				
		1% duty)				

* See attached radiation budget form

The beam energies, E_{Beam}, available are: $E_{Beam} = N \times E_{Linac}$ where N = 1, 2, 3, 4, or 5. E_{Linac} = 800 MeV, i.e., available E_{Beam} are 800, 1600, 2400, 3200, and 4000 MeV. Other energies should be arranged with the Hall Leader before listing.

HAZARD IDENTIFICATION CHECKLIST

JLab Proposal No.: _____ Date: Dec 16, 1998
(For CEBAF User Liaison Office use only.)

Check all items for which there is an anticipated need.

Cryogenics
- _____ beamline magnets
- _____ analysis magnets
- _____ target
  - type: _____
  - flow rate: _____
  - capacity: _____

Electrical Equipment
- _____ cryo/electrical devices
- _____ capacitor banks
- _____ high voltage
- _____ exposed equipment

Radioactive/Hazardous Materials
List any radioactive or hazadorous/ toxic materials planned for use:
_____
_____
_____
_____

Pressure Vessels
- _____ inside diameter
- _____ operating pressure
- _____ window material
- _____ window thickness

Flammable Gas or Liquids
- type: _____
- flow rate: _____
- capacity: _____

Drift Chambers
- type: _____
- flow rate: _____
- capacity: _____

Other Target Materials
- ✓ Beryllium (Be)
- ___ Lithium (Li)
- ___ Mercury (Hg)
- ✓ Lead (Pb)
- ___ Tungsten (W)
- ___ Uranium (U)
- ___ Other (list below)

_____
_____

Vacuum Vessels
- _____ inside diameter
- _____ operating pressure
- _____ window material
- _____ window thickness

Radioactive Sources
- _____ permanent installation
- _____ temporary use
- type: _____
- strength: _____

Large Mech. Structure/System
- _____ lifting devices
- _____ motion controllers
- _____ scaffolding or
- _____ elevated platforms

Lasers
- type: _____
- wattage: _____
- class: _____

Installation:
- _____ permanent
- _____ temporary

Use:
- _____ calibration
- _____ alignment

Hazardous Materials
- ___ cyanide plating materials
- ___ scintillation oil (from)
- ___ PCBs
- ___ methane
- ___ TMAE
- ___ TEA
- ___ photographic developers
- ___ other (list below)

_____
_____

General:

Experiment Class:
- _____ Base Equipment
- _____ Temp. Mod. to Base Equip.
- _____ Permanent Mod. to Base Equipment
- _____ Major New Apparatus

Other: _____
_____

LAB RESOURCES LIST

JLab Proposal No.: _____ Date Dec 16, 1998
(For JLab ULO use only.)

List below significant resources — both equipment and human — that you are requesting from Jefferson Lab in support of mounting and executing the proposed experiment. Do not include items that will be routinely supplied to all running experiments such as the base equipment for the hall and technical support for routine operation, installation, and maintenance.

Major Installations *(either your equip. or new equip. requested from JLab)*

1. Septum Magnets
2. Total absorption detector
3. ^{208}Pb target

New Support Structures:

1. Structure to mount detector (similar to HAPPEX expt)

Data Acquisition/Reduction

Computing Resources:

New Software:

Major Equipment

Magnets: septum magnets

Power Supplies:

Targets: ^{208}Pb target

Detectors: quartz-tungsten total absorption detector

Electronics:

Computer Hardware:

Other:

Other:

MEMORANDUM
To: Bob Michaels
From: Pavel Degtiarenko
Subj: radiation budget
cc: R. May
Date: December 4, 1998

Radiation budget form for the proposed experiment

The estimates for the boundary radiation dose from the proposed experiment are given in the attached spreadsheet. The calculations do not take into account the new septum magnet.

The boundary dose accumulation due to this experiment is estimated to be 2.2 mrem, i.e. 22% of the annual design goal limit. The dose rate averaged over the run time is approximately 3 times larger than the allowed average dose rate, which makes this experiment subject to further scrutiny. The dose rates inside the hall I expect will be comparable with other typical low energy/thick target setups.

Hall: A

RADIATION BUDGET FORM

Exp. # Exx-xxx **rev:** **run dates: 1998-99** **name of liaison: Bob Michaels**

				totals:
setup number			1	
beam	energy	GeV	0.850	
	current	uA(CW)	50.0	
exp't target	element		Pb208	
	thickness	mg/cm2	637	
time	run time (100% eff.)	hours	700	700
		days	29.2	29.2
	installation time	hours		0
		days	0.0	0.0
dose rate at the fence post (run time)	method 1	urem/hr	3.25	
	method 2	urem/hr		
	conservative	urem/hr	3.25	
dose per setup		urem	2272.8	2272.8
% of annual dose budget		%	22.728	22.728
			% of allowed dose for the total time	284.42
			% of allowed dose for the run time only	284.42

If > 200%, discuss result with Physics Research EH&S officer

date form issued: December 3, 1998 *authors:* P Degtyarenko, R Royenko

Proposal to Jefferson Lab PAC 15

A CLEAN MEASUREMENT OF THE NEUTRON SKIN OF ^{208}Pb THROUGH PARITY VIOLATING ELECTRON SCATTERING

R. Michaels and P.A. Souder, Spokesmen

P.A. Souder, R. Holmes
Syracuse University

J.M. Finn, T. Averett, D. Armstrong
College of William and Mary in Virginia

R. Carlini, J.P. Chen, E. Chudakov, K. De Jager, J. Gomez, M. Kuss, J. LeRose, M. Liang, R. Michaels, J. Mitchell, A. Saha, B. Wojtsekhowski
Thomas Jefferson National Accelerator Facility

E. Burtin, C. Cavata, D. Lhuillier, F. Marie, T. Pussieux
DSM/DAPNIA/SPhN CEA Saclay

M. Amarian, E. Cisbani, S. Fullani, F. Garabaldi, M. Iodice, R. Iommi
INFN/Rome

R. De Leo
INFN/Bari

A. Leone, R. Perrino
INFN/Lecce

G.D. Cates, B. Humensky, K. Kumar
Princeton University

J. Calarco, W. Hersman
University of New Hampshire

P. Markowitz
Florida International University

(This is a Hall A Collaboration Proposal)

ABSTRACT

The difference between the neutron radius R_n of a heavy nucleus and the proton radius R_p is believed to be on the order of several percent. This qualitative feature of nuclei, which is essentially a neutron skin, has proven to be elusive to pin down experimentally in a rigorous fashion. We propose to measure the parity-violating electroweak asymmetry in the elastic scattering of polarized electrons from ^{208}Pb at an energy of 850 MeV and a scattering angle of 6°. Since the Z_0 boson couples mainly to neutrons, this asymmetry provides a measure of the size of R_n with respect to R_p that can be interpreted with as much confidence as traditional electron scattering data. The projected experimental precision corresponds to a ± 1 % determination of R_n, sufficient to establish the existence of the neutron skin if it is of the expected size.

A Clean Measurement of the Neutron Skin of ^{208}Pb Through Parity Violating Electron Scattering

I INTRODUCTION

The neutron radius R_n in ^{208}Pb is generally assumed to be about 0.25 fm larger than the proton radius $R_p \sim 5.5$ fm. This "neutron skin" is a fundamental qualitative feature of nuclear structure characteristic of all large nuclei that has unfortunately never been cleanly observed.

In contrast, the proton radius of the nucleus can be cleanly measured by, for example, electron scattering or the spectroscopy of muonic atoms. The interpretation of this data is more complex than the usual textbook analysis using plane waves and the Born approximation. However, reliable calculations using accurate solutions of the Dirac Equation can be done.

Determining the neutron radius of the nucleus is more complex. Electron scattering from neutrons is primarily magnetic and thus does not directly measure the neutron density. Hence hadronic probes such as pions and protons must be used, and the interpretation of the data has serious theoretical difficulties at the desired level of precision. Our opinion, based on private conversations and reading the literature, is that the uncertainty in the neutron radius is at present 5%, if not larger. We feel that it is extremely important to reduce this error to the 1% level so that we can definitively state whether or not this feature of nuclei exists. This experiment has the potential to be a benchmark for nuclear physics in the same way that charge density measurements established our picture of the size and shapes of nuclei about 15 years ago.

One possible clean way to measure the neutron skin is to use the weak interaction. The Z-boson in the Standard Model couples primarily to the neutron, and can be used to determine the neutron radius with the same level of confidence that electromagnetic probes determine R_p. Some time ago, it was pointed out that parity-violation in the elastic scattering of polarized electrons is a practical method for using the Z to determine neutron radii [1]. Recently, a realistic calculation of the asymmetries, taking into account the distortion of the electron wavefunctions, has been published [2].

Based on the results of Ref. [2], we have designed an experiment to measure R_n. It requires measuring the parity-violating amplitude in elastic $\vec{e}$–^{208}Pb scattering at the 3% level. The experiment will be sensitive to the R_n at the 1% level, ample to establish presence of the neutron skin.

II THEORY

A Knowledge of Neutron Radii

The "neutron skin" is potentially a fundamental feature of heavy nuclei. The important question that we address here is exactly what empirical basis we have at present for accepting the existence of this feature. The most detailed published discussion of this issue, by Pollock, Fortson, and Wilets (PFW) [**3**], was written in the somewhat interdisciplinary context of using parity violation in heavy atoms as a test of the Standard Model. It turns out that the answer is not simple. The information on the neutron radius is somewhat indirect, comes from many sources, and depends on theoretical input with uncertainties that are hard to pin down. As a result, there are not many published estimates of the total error in R_n. A paper by Fortson *et al.*[**4**] suggests $\delta R_n \sim 10\%$. There are probably also experts in the field that would quote an error at the level of 3% or less.

To illustrate some of the issues, we will briefly review how R_n is determined, following the discussion of PFW. One source of information comes form Hartree-Fock calculations based on phenomenological potentials that reproduce a large body of data. The main goal of our experiment is to constrain these parameters. A summary of relevant calculations as given in by PFW is reproduced in the following table:

Table I:
Values of R_n/R_p from Hartree-Fock calculations as given in PFW. Also given is the quantity q_n, which, as will be explained below, is a parameter in the computation of the effect of parity violation in lead atoms.

	R_n/R_p	q_n
G:HFB	1.025	0.90260
SkA	1.039	0.90051
Sk*	1.031	0.90176
Sk3	1.023	0.90334
Rel	1.056	0.89813

The spread in the calculations of R_n/R_p is seen to be 0.03. If one assumes that the spread is random, a σ of 0.1 is obtained; the error in the average is even smaller. However, the assumption of random errors in R_n/R_p is inappropriate. The relevant question is *how much can R_n/R_p be changed without losing the other successes of the calculation ?* There is no published answer to this question, but accommodating changes in R_n/R_p of 0.05 or more is plausible [3]. We conclude that the Hartree-Fock calculations, even with their many successes, do not conclusively establish the existence of the neutron skin.

Another published error on the thickness of the neutron skin appears in a paper on scattering experiments. The result, using data on the scattering of polarized protons from ^{208}Pb, is an impressive value $R_n - R_p = 0.14 \pm 0.04$ fm (relative to $R_p \sim 5.45$ fm) [5]. However, PFW states that there are additional theoretical uncertainties arising from the hadronic nature of the proton as a probe that add considerable error. Moreover, the value for $R_n - R_p$ exhibits a large and unphysical dependence on the energy of the beam used for the experiment [5], as shown in Fig. 1.

Data comparing the elastic scattering of positive and negative pions exist [6], but again there are uncertainties in the analysis. [3] These methods are not really directly sensitive to the neutron distribution.

The method of using parity violation described in this proposal is directly sensitive to the neutron radius. The uncertainties in the theoretical interpretation of the results (discussed in more detail below) are expected to be much smaller than the problems just discussed. If we can achieve our projected experimental error and if the neutron skin is of the expected thickness, we can cleanly establish its existence.

B Summary of Physics Motivation

Based on the discussion of the state of our understanding of the neutron skin stated above, we are motivated to do our experiment for the following reasons:

1. Establish the existence of the neutron skin. This is a rather striking feature of nuclei which has not been definitely established. This is a most unsatisfactory situation for a field as mature as ours.

2. If the size of the neutron skin is different than presently assumed, it will require significant changes in the parameters of the effective potentials used in the Hartree-Fock calculations. This might have quite broad impact. One example cited by Horowitz is computations of astrophysical interest on unstable asymmetric nuclei [2].

3. Determine a value of R_n suitable for tests of the Standard Model that use parity violation in atoms. The success of our measurement will provide additional encouragement of the atomic experiment in progress. Moreover, our experiment will make atomic experiments on a single isotope easier to interpret. The single-isotope experiments are easier than the alternative approach of trying to precisely measure the N-dependence of various isotopes.

C Parity Violation in Heavy Atoms

The neutron radius is also important for precise studies of parity violation in atomic physics. The reason is as follows. The solution of the Dirac equation for the naive potential of uniform charge density for $r < R$

$$V(r) = Ze^2 \times \left\{ \begin{array}{ll} (-3 + r^2/R^2)/2R & r < R, \\ -1/r & r > R. \end{array} \right\} \tag{1}$$

normalized to unity at the origin, is

$$f(r) = 1 - \frac{1}{2}(Z\alpha)^2 \left[\left(\frac{r}{R}\right)^2 - \frac{1}{5}\left(\frac{r}{R}\right)^4 + \frac{1}{75}\left(\frac{r}{R}\right)^6 \right] \tag{2}$$

At the surface, $f(r)$ has changed by ~20%. The average of $f(r)$ is

$$q_n = \int \rho_n(r) f(r) d^3r \sim 1 - \frac{3}{70}(Z\alpha)[1 + 5R_n^2/R_p^2] \sim 0.9 \tag{3}$$

as shown in Table I. Here $R_{p(n)}$ is the proton(neutron) radius. The difference between q_n and unity is approximately proportional to $(R_n/R_p)^2$ if it is assumed that the neutron density is approximately constant and if $R_n \sim R_p$. Without these assumptions, more information about the shape of the neutron density is needed. However, the values for q_n shown above in Table I. for all the calculations are linearly related, suggesting that measuring a single parameter is sufficient at the needed level of precision.

The atomic parity-violating amplitudes are approximately proportional to q_n. The experimental error in the atomic experiment on Cs is presently at the 0.3% level. The atomic theory is uncertain at the 1% level, which is larger than the error in q_n. However, extensive work is underway to improve the atomic physics experiments using a variety of new techniques. The atomic calculations are expected to be feasible at the required level of precision. Hence, we believe that our measurement of R_n will become important to this field.

D Parity-Violation and the Neutron Radius

The potential between an electron and a nucleus may be written

$$\hat{V}(r) = V(r) + \gamma_5 A(r) \tag{4}$$

where the usual electromagnetic vector potential is

$$V(r) = \int d^3r\prime Z\rho(r\prime)/|\vec{r} - \vec{r}\prime| \tag{5}$$

and where the charge density $\rho(r)$ is closely related to the point proton density $\rho_p(r)$ given by

$$Z\rho_p(r) = \sum_p \langle \psi_p^\dagger(r)\psi_p(r)\rangle. \tag{6}$$

The axial potential $A(r)$ depends also on the neutron density:

$$N\rho_n(r) = \sum_p \langle \psi_n^\dagger(r)\psi_n(r)\rangle. \tag{7}$$

It is given by

$$A(r) = \frac{G_F}{2^{3/2}}[(1 - 4\sin^2\theta_W)Z\rho_p(r) - N\rho_n(r)] \tag{8}$$

The axial potential has two important features:

1. It is much smaller than the vector potential, so it is best observed by measuring parity violation.
2. Since $\sin^2\theta_W \sim 0.23$, $(1 - 4\sin^2\theta_W)$ is small and $A(r)$ depends mainly on the neutron radius $\rho_n(r)$.

The cross section for scattering electrons with momentum transfer squared Q^2 is given by

$$\frac{d\sigma}{d\Omega} = \frac{d\sigma}{d\Omega}_{\text{Mott}} |F_p(Q^2)|^2 \tag{9}$$

where

$$F_p(Q^2) = \frac{1}{4\pi}\int d^3r j_0(Qr)\rho_p(r) \tag{10}$$

is the form factor for protons.

One can also define a form factor for neutrons

$$F_n(Q^2) = \frac{1}{4\pi}\int d^3r j_0(Qr)\rho_n(r) \tag{11}$$

By scattering polarized electrons, one can measure the parity-violating asymmetry which is the interference term between $V(r)$ and $A(r)$

$$A_{LR} = \frac{\sigma_R - \sigma_L}{\sigma_R + \sigma_L}, \tag{12}$$

where $\sigma_{L(R)}$ is the cross section for the scattering of left(right) handed electrons. The result is

$$A_{LR} = \frac{G_F Q^2}{4\pi\alpha\sqrt{2}}\left[1 - 4\sin^2\theta_W - \frac{F_n(Q^2)}{F_p(Q^2)}\right] \tag{13}$$

Thus A_{LR} is approximately proportional to the ratio of neutron to proton form factors.

This low Q^2 measurement is strongly related to the root mean square radius of the neutron distribution. However, there is a small dependence on the shape of the density in addition to its radius. We emphasize that this model dependence is not a problem for comparing to theory. We are measuring a well-defined form factor of the neutron radius at this Q^2. Theoretical models can simply calculate this form factor for a direct comparison with experiment.

E Realistic Calculations

The above analysis assumes plane waves for the electrons. For heavy nuclei such as Pb, this is a poor approximation. Hence the analysis must be done for scattering states that are solutions to the Dirac Equation

$$[\alpha \cdot \mathbf{p} + \beta m_e + \hat{V}(r)]\psi = E\psi \tag{14}$$

valid when $Z\alpha$ is relatively large. This has been done by Horowitz [**2**].

There are three vital questions about the realistic solution:

1. How large are the effects of the distortions on the asymmetries ?
2. How sensitive are the asymmetries to the neutron radius ?
3. How precise are the calculations ?

The distortions are substantial, as shown in Fig. 2, typically on the order of 20%, but vary strongly with Q^2. At certain values of Q^2 the asymmetries depend strongly in the neutron radius. There is a point below the first diffraction dip where a 3% measurement of A_{LR} yields the desired 1% measurement of the neutron radius.

The calculations are precise enough to support the experiment. The numerical accuracy of the code ELASTIC.FOR used in ref [2] is expected to be significantly better than 1% for the asymmetry at the proposed kinematics. This code passes a number of stringent tests that give us confidence in the results: cross sections are reproduced over the full range of momentum transfers for existing ^{208}Pb data. The large angle cross section is numerically more demanding than the forward angle asymmetry. Next, the plane wave asymmetry results were reproduced by simply running the full code with small potentials. Finally, subtraction between positive and negative helicity states needed for the asymmetry was tested by running the full code with the value of G_{Fermi} 100 times *smaller* than its true value and scaling the asymmetry by 100. This makes the subtraction 100 times more sensitive.

One important question is how do we measure R_n with a measurement at a single Q^2 value? This is well known to be impossible for electron scattering. However, we make the reasonable assumptions that:

1. The normalized neutron and proton densities are approximately the same.
2. The difference is described to first order in R_n.

At our value of Q^2, we are predominantly sensitive to R_n and only slightly sensitive to other shape parameters. Thus it would take a rather bizarre difference in shapes between the proton and neutron densities to cloud the interpretation.

F Choice of Nucleus

There are two nuclei that are attractive for our measurement, Pb and Ba. They are both equally accessible experimentally. Pb has the advantage that it is very well studied. Ba has the advantage that it is one of the nuclei being used for an atomic physics test of the Standard Model. However, in the spirit that the major unknown feature involves only a single parameter in the nuclear potential, this effect can be computed reliably for any nucleus once a good measurement is done on another nucleus. Given no strong theoretical prejudice, we have chosen Pb as the more convenient nucleus.

III EXPERIMENTAL DESIGN

A Overview

This experiment will run at a beam energy of 850 MeV and use a 6° scattering angle. The two identical 3.7 msr septum magnet + HRS spectrometers will focus elastically scattered electrons into total-absorption detectors in their focal planes. A 50μA, 80% polarized beam with a 30 Hz helicity reversal frequency line locked to the 60 Hz frequency of AC power will be used. The helicity will be structured into pairs of 33.3 msec periods of opposite helicity, where the sign of the helicity of the first in the pair is determined pseudorandomly. Much of the experimental technique used in the HAPPEX experiment will be used [**7**]. Ratios of detected flux to beam current integrated in the helicity period are formed, and the parity violating asymmetry in these ratios computed from the helicity correlated difference divided by the sum: A = (σ_R - σ_L) / (σ_R + σ_L), where $\sigma_{R(L)}$ is the ratio for right(R) an left(L) handed electrons.

B Choice of Kinematics

The choice of kinematics is guided by maximizing the figure of merit, defined as $R \times A^2 \times \epsilon^2$, where R is the detected scattered rate, A is the asymmetry, and ϵ is the required accuracy. Note that the figure of merit defined in this way is the correct quantity to optimize because it takes into account simultaneously the rate, asymmetry, and the required accuracy. The required accuracy is determined by the sensitivity of the parity violating asymmetry to the neutron radius. Figure 2 shows the asymmetry for ^{208}Pb calculated by Horowitz [**2**]. Also shown is the fractional deviation in the asymmetry $(A1 - A)/A$ for the the case of a neutron radius stretched by 1% ($A1$) compared to unstretched (A). Taking $\epsilon = (A1 - A)/A$, we obtain the figure of merit F.O.M. $= R \times (A1 - A)^2$. The rates and asymmetries that we expect to be detected by a focal plane detector were computed using a computer code whose ingredients were: 1) Asymmetries taken from tabulated results provided by Horowitz. These results were calculated for each bin in energy and angle. 2) Optical properties and resolutions taken from the design report on the septum magnet + HRS. These properties are not very different from the established HRS properties. The asymmetry was then averaged over the acceptance, which has a nontrivial effect on the optimization since the cross section varies strongly. 3) Some assumptions about the radiative losses and

heat load capacity of the target, as explained later.

In figure 3 we show how the F.O.M. varies with the electron beam energy and scattering angle. For the septum magnet at 6 degrees, the maximum F.O.M. occurs at $E \approx 850$ MeV. Thus, with the forward angles allowed by the septum magnet, the optimum energy for the experiment is uniquely determined, and it happens to be a natural energy for Jefferson Lab. Intuitively, this optimum occurs because while the asymmetry grows with Q^2 the cross section drops. In these kinematics, a 3% accuracy for the asymmetry is required to make a 1% measurement of the neutron radius.

This feasibility study was repeated for ^{137}Ba using the same technique, for which the optimum energy turned out to be 1 GeV, again a JLab energy. The asymmetry is bigger and the rate smaller; the net effect on running time is that it is 7% longer for Ba than for the case of Pb. As was explained in the section II.F, we have chosen lead as the more convenient target.

C Detected Rates and Asymmetry

The distribution of rates and asymmetries in the focal plane are shown in figure 4. The first excited state of ^{208}Pb is at 2.6 MeV and could be discriminated by the high resolution of the spectrometers, but we will instead choose to integrate up to 4 MeV to catch a good fraction of the radiative tail and increase the rate. (See the next section for a discussion of the correction due to the excited states.) The rates are high, 860 MHz. A total absorption detector made of quartz-tungsten will be constructed to integrate the elastically scattered electrons. A similar detector is under construction for experiment E158 at SLAC where it is designed for a similar purpose and where it will be able to take four times the rate at 20 times the beam energy for four times the running time. Table 1 shows the rates, asymmetries, and running times. A target of "effective" thickness 3.7% of a radiation length was assumed as explained in the next section.

We provide here a simple estimate of the counting rates for purposes of illustrating how we arrive at a beam time estimate of 30 days. We emphasize that the code used to compute the asymmetry and rates did average over the finite acceptance. Nevertheless, the following estimate provides approximately the correct answer. We assume that our errors are dominated by counting statistics. We will measure an asymmetry:

$$A = \frac{N_+ - N_-}{N_+ + N_-} \tag{15}$$

TABLE 1. Acceptance Averaged Rate and Asymmetry

Measured Asymmetry (p_e A)	0.51 ppm
Beam Energy	850 MeV
Beam Current	50μA
Required Accuracy	3%
Energy Cut (due to detector)	4 MeV
Detected Rate (ea spectrometer)	860 MHz
Running Time	690 hours

$$\text{with } N = N_+ + N_- \qquad N_+ \approx N_- \tag{16}$$

$$\text{The error is} \qquad \delta A = \frac{1}{\sqrt{N}} \tag{17}$$

Given 30 days of beam time, we detect a number of scattered electrons

$$N = \frac{d\sigma}{d\Omega} \times \Delta\Omega \times tgt \times I \times T \tag{18}$$

where the cross section, solid angle, target thickness, beam current, and running time are

$$\frac{d\sigma}{d\Omega} \approx 1100 \text{ mb/sr} \tag{19}$$

$$\Delta\Omega = 2 * 3.7 \text{ msr} = 0.0074 \text{ sr} \quad -- \text{ solid angle of 2 spectrometers} \tag{20}$$

$$tgt = \text{eff. target thickness} \approx 3.7\% \; RL = 0.23 \text{ g/cm}^2 = 6.6 \times 10^{20} \text{atoms/cm}^2$$

$$I = 50 \; \mu A = 3.1 \times 10^{14} \text{ electrons / sec} \tag{21}$$

$$T = 690 \text{ hours } (\approx 30 \text{ days}) = 2.5 \times 10^6 \text{ sec} \tag{22}$$

The result is $N \approx 4.1 \times 10^{15}$ particles leading to $\delta A = 0.016$ ppm. We want to measure $A_{\text{physics}} = 0.64$ ppm with 80% polarization beam, i.e. $A_{\text{raw}} = 0.51$ ppm. We therefore arrive at 3% accuracy in the asymmetry for 30 days of running. The acceptance–averaged result is similar.

TABLE 2. Error Budget

Source of Error	$\frac{\Delta A}{A}$ (%)
Polarization	1.0
Q^2 Determination	0.5
Finite Acceptance	0.3
Beam Systematics	0.2
Backgrounds	0.2
Total Systematic Error	1.2
Statistics	3.0
Total Experimental Error	3.2

D Error Budget

The experimental errors which we will need to achieve are given in table 2. It will probably be necessary to use the Møller polarimeter after first calibrating it with the Compton polarimeter, as well as the Hall C polarimeter and 5 MeV Mott polarimeter. The experiment's demands on the alignment accuracy, knowledge of acceptance, and calibration of the spectrometers including the septum magnets are within design specifications. The main issue is measuring the Q^2, and we are not measuring an absolute cross section. Knowledge of the beam systematics will have to be established at a level a factor of $\approx$10 better than the conservative upper bound already established in the initial HAPPEX experiment; much of the beam study can be done parasitically. The backgrounds, including inelastic contributions and scattering from magnetized iron, will need to be controlled. Simulations, as well as analysis of early data from the septum magnet runs, will be required.

E Target Design

Considerations of the target design has involved the following factors.

1. Optimizing the thickness and geometry of the target.
2. Improving the thermal properties of the target, which is necessary since a simple lead target will melt in a high beam current.
3. Boundary radiation in the hall.
4. Influence of the inelastic states.

5. When using a "cooling agent" to improve the thermal properties of the target, such as a helium gas jet or a mixture of beryllium in the lead target, we must compute the influence of this agent on the measurement.

As explained below, if the target is a single foil, a thickness of $\approx$10% of a radiation length (RL) gives the maximum detected rate in our detector, where the upper limit is determined by radiative losses. For running a target this thick, one must also consider the radiation deposited in the hall – both the instantaneous and the integrated radiation. Calculations [8] show a boundary dose of about 2.2 mrem which is 22% of the annual design goal limit. The instantaneous dose, however, is about 3 times higher than the allowed average dose rate, and we may need to reduce this with local shielding. A target much thicker than 10% RL therefore seems impractical. A design to use multiple foil targets would increase the rates, and this also introduces some nontrivial corrections which we have not yet calculated. In conclusion, since a single foil is much simpler, and since a 10% RL seems to be a practical maximum, all discussion here assumes a single foil.

Concerning radiative corrections, we note that they mainly have the effect of reducing our rate by kicking electrons out the focal plane detector. Otherwise, radiative corrections are not a significant source of systematic error for the experiment because the spectrometer resolution is better than 1% and the electroweak radiative corrections can be calculated reliably at this level.

The maximum "effective" thickness of the target is determined from the energy loss cut imposed by the detector in the focal plane and the Brehmsstrahlung radiative losses in the target. The effective thickness is defined as the product of the actual thickness times the fraction of elastic events which make it into the detector, calculated at the value of actual thickness where this product is maximum. The effective thickness is a maximum for an actual thickness of $\approx$10% RL. In figure 5 we show how the effective thickness varies with the energy cut. With a cut at 4 MeV, we can get an effective thickness of 3.7% RL. If the cut is at 2 MeV, as required to discriminate the first inelastic state of lead at 2.6 MeV, the effective thickness is 2.8% RL.

By adding the rate up to 4 MeV, we reduce the running time by 25%, but the price to pay is that we must compute the systematic uncertainty due to the inelastic states. The systematic uncertainty is estimated as follows. This part of the discussion is general and pertains to any process that contaminates our signal. The measured asymmetry will be will be

$$\frac{\sum_j D_j \epsilon_j}{2 \sum_k (d\sigma/d\Omega)_k \epsilon_k}$$

where the sum is over the various incoherent processes, D is the parity violating difference in the cross section, ϵ is the efficiency for detecting the process, and $d\sigma/d\Omega$ is the cross section. Therefore, for this correction we need to know the fraction of contamination from the process and its electroweak asymmetry. Then the systematic error is, by definition, the error in this correction. Ideally the correction should be negligible also.

The inelastic states up to 4.3 MeV add up to a very small 0.5% of the elastic scattering rate. Therefore, even if the asymmetries for these inelastic states were different from the asymmetry for elastic scattering by 100%, they would represent a $\leq$1% systematic error. The main contribution comes from the first excited state at 2.6 MeV. This is a collective state, and the electroweak asymmetry was estimated by Horowitz **[9]** to be 25 $\pm$ 35% larger than the asymmetry for elastic scattering. The correction to our measurement is negligible. We've assumed a cut of 4 MeV in our calculations. Errors induced due to impurities in the lead after isotope separation can be estimated. The errors induced by ^{9}Be or ^{4}He "cooling agents" have been estimated, as described later.

The power dissipated in the ^{208}Pb target will be about 60 Watts for a 50 μA beam. A calculation of the temperature distribution **[10]** for a 2 mm raster pattern shows that with simple water-cooling of the four edges we could sustain $\approx 20\mu$A. Our target design for improving the heat capacity is shown in figure 6 and is still being engineered. The design will contain some, and possibly all, of the following ingredients in addition to beam rastering:

1. A lead-beryllium alloy, or possibly a set of lead and beryllium foils pressed together, will be deployed. The beryllium improves the thermal conductivity, and since it has low Z, a reasonable mixture can be made that contributes $\leq$5% to our signal. This systematic is discussed further below.

2. The lead (or lead-beryllium) will be mounted on a wheel and rotated, as shown in fig 6. The wheel will rotate through the beam much faster than the characteristic time scale for heating the beam spot region to the melting point. This is a known technique for lead targets.

3. A helium gas jet will cool the target. For a spinning target design, the beam enters in the bottom part of the orbit, and the helium cools the top part. We have calculated that a helium gas jet with a reasonable flow rate, over a fraction of about 1/4 of the area of the disk, could provide significant cooling of order 50 Watts. Further heat dissipation occurs through the bearings and the water–cooled axle.

An important consideration in the target design is the noise induced by rastering or spinning. The helicity–pair error in the asymmetry due to counting statistics will be 1.4×10^{-4} for lead, and all other noises must be smaller. The best that can be achieved in the uniformity of foil thickness is of order 1%. In addition, the noise induced by rastering is also of order 1%. We plan to achieve a cancellation of the foil–thickness noise by rotating the target at a frequency synchronized to the helicity flipping frequency 30 Hz. With a 3 Hz frequency of rotation, helicity pairs from angular segments of $2\pi/10$ radians of rotation angle will be matched. The raster frequency is a factor of 600 times faster than the helicity flipping frequency, and the repetition of orbits should cancel the raster noise at the required level of accuracy. We note that it seems likely that spinning the target is not necessary to achieve the heat load capability, thus we would avoid this potential noise problem.

Finally we mention the systematic error due to using ^{9}Be and ^{4}He as "cooling agents". One reason these were chosen is that they have low Z and therefore do not contribute much signal. Calculations of rates for reasonable levels of contamination (e.g. 0.1 mm of ^{9}Be) show that the rates of $\leq$5% of the ^{208}Pb rate are achievable. For such a mixture of ^{9}Be and ^{208}Pb, the thermal conductivity and melting point are increased. One also needs to know the electroweak effects from these nuclei. In the case of ^{4}He, which has $J^\pi T = 0^+0$, this is well–known and is to a good approximation independent of nuclear structure. In the case of ^{9}Be we have estimated the parity violating asymmetry for elastic scattering using the shell model. In addition, since we are at forward angle and since the axial–hadronic coupling is small, it turns out one may get a reasonably accurate cross check of the asymmetry of ^{9}Be model independently using the low-Q^2 expansion of the electromagnetic multipole matrix elements in terms of measured electrostatic properties of the nucleus. In summary, the electroweak asymmetries of ^{4}He and ^{9}Be "cooling agents" can be computed to at least 25% accuracy, their contributions are smaller than our experimental error, and they introduce negligible systematic error.

F Other Experimental Considerations

Apart from the new target and the high rates that will appear in the spectrometer detector hut, this experiment should make few new demands on the lab infrastructure, though the precision required is certainly challenging. The planned and approved septum magnet system will be used. We already have excellent information about the backgrounds of the HRS, from data analysis and simulation, which were applied to the HAPPEX experiment. A similar analysis will be carried out for the septum magnet + HRS system prior to

running this experiment. We believe we can measure Q^2 to better than 0.5%.

Hall A at Jefferson Lab is the best place to run this experiment. Given the forward-angle capabilities of the septum magnet we have shown that 850 MeV is the best energy, which is a natural 1-pass beam at JLab. Furthermore, the projected $\approx$2% accuracy of the Hall A Compton polarimeter will be useful for cross checking the Møller polarimeter. The excellent stability and quality of the JLab beam allowed us to make systematic–free measurements of parity violation in HAPPEX [7], and will be crucial for this proposal. This experiment would be much more difficult at a pulsed machine like Bates. The experience and knowledge–base of the polarized injector group, lab staff, and collaboration are also important factors in making a measurement with 10^{-8} error.

Techniques in the production of polarized beam, accurate measurement of polarization, diagnostics of beam systematics, and other systematics will be quite similar to what has either already been achieved in the HAPPEX experiment or will be achieved in the next few years. We can use the same DAQ as HAPPEX, with a few upgrades. It has been demonstrated that parity violation experiments with systematic errors of 2×10^{-8} in electron scattering are feasible [11], and based on our experience with HAPPEX, we believe Jefferson Lab is also capable of such accuracy.

IV BEAM TIME REQUEST

We request 690 hours of production running with 50μA of 80% polarized beam. In addition, we'll need 20 hours of time for setup and checkout as explained below. The total time is 710 hours or 30 days.

We plan to study the systematics of the strained GaAs polarized beam parasitically; indeed this work has already begun. The strained GaAs is likely to be a significant challenge for controlling helicity correlated systematics. If successful, these beam studies will demonstrate that the beam and beam line instrumentation are adequate. Systematics associated with the beam are among the most difficult and subtle problems for parity violation experiments.

We will participate in the commissioning of the septum magnet and will use data from that commissioning as well as early experiments to examine issues of acceptance, systematics of alignment, accuracy of Q^2, backgrounds, and pole–tip scattering. Prior to our production run, we'll need to set up the septum magnet. Assuming the septum magnet is installed, we need about 20 hours of additional setup and checkout time to align the detector and measure Q^2. Some facility development time will be needed to verify that our target works and has good noise characteristics.

V REFERENCES

1 T.W. Donnelly, J. Dubach, and I. Sick, Nucl. Phys. **A503**, 589 (1989).
2 C. J. Horowitz, Phys. Rev. C **57**, 3430 (1998).
3 S.J. Pollock, E.N. Fortson, and L. Wilets Phys. Rev. C **46**, 2587 (1992).
4 E.N.Fortson, Y. Pang, and L. Wilets, Phys. Rev. Lett. **65**, 2857 (1990).
5 L.Ray and G.W.Hoffmann, Phys. Rev. C **31**, 538 (1985).
6 C. Olmer *et. al.*, Phys. Rev. C **21**, 254 (1980)
7 HAPPEX Collaboration, paper recently submitted to PRL.
8 P. Degtiarenko, memo on radiation budget.
9 C.J. Horowitz, private communication.
10 C. Cothran, memo on solid target heating.
11 P.A. Souder *et al.*, Phys. Rev. Lett. **65** 694 (1990).

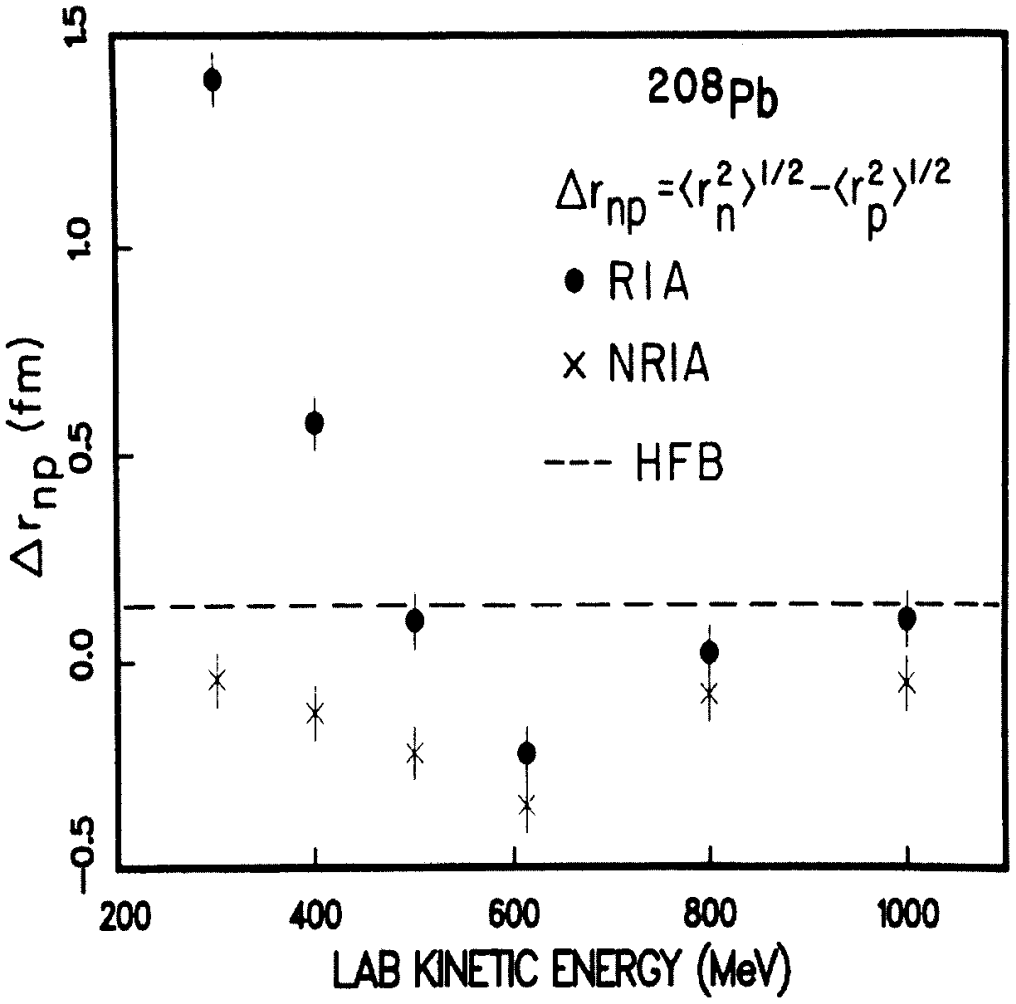

FIGURE 1. Neutron-proton rms radii differences for ^{208}Pb deduced from proton nucleus elastic scattering using RIA (solid dots) and the first order NRIA (crosses). The theoretical Hartree-Fock-Bogoliubov (HFB) value is indicated by the dashed line. This figure is taken from reference [5] where it is called fig. 10.

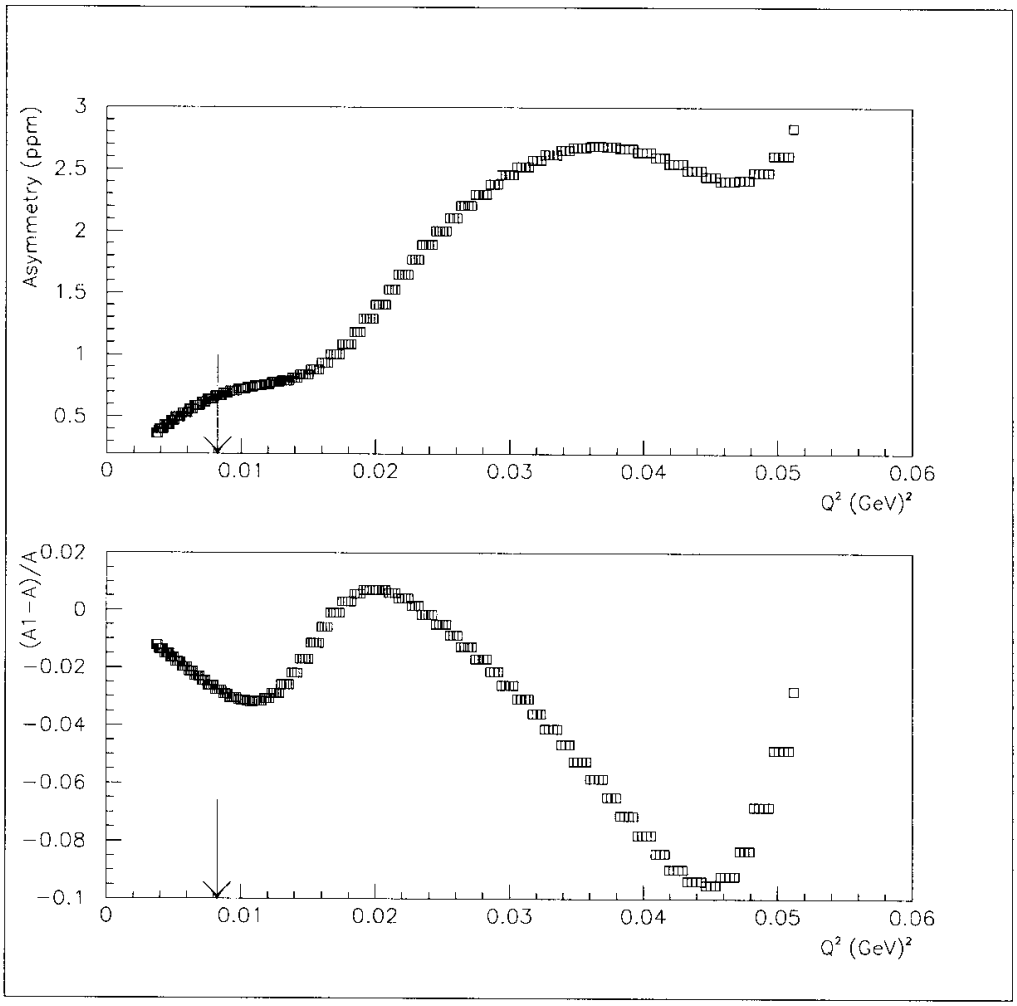

FIGURE 2. Top figure: Asymmetry for ^{208}Pb versus Q^2 at the energy where the figure of merit is maximum. Bottom : The fractional deviation $(A1 - A)/A$, where $A1$ is the asymmetry for a 1% stretched neutron radius and A is unstretched. The chosen Q^2 is indicated by the arrow.

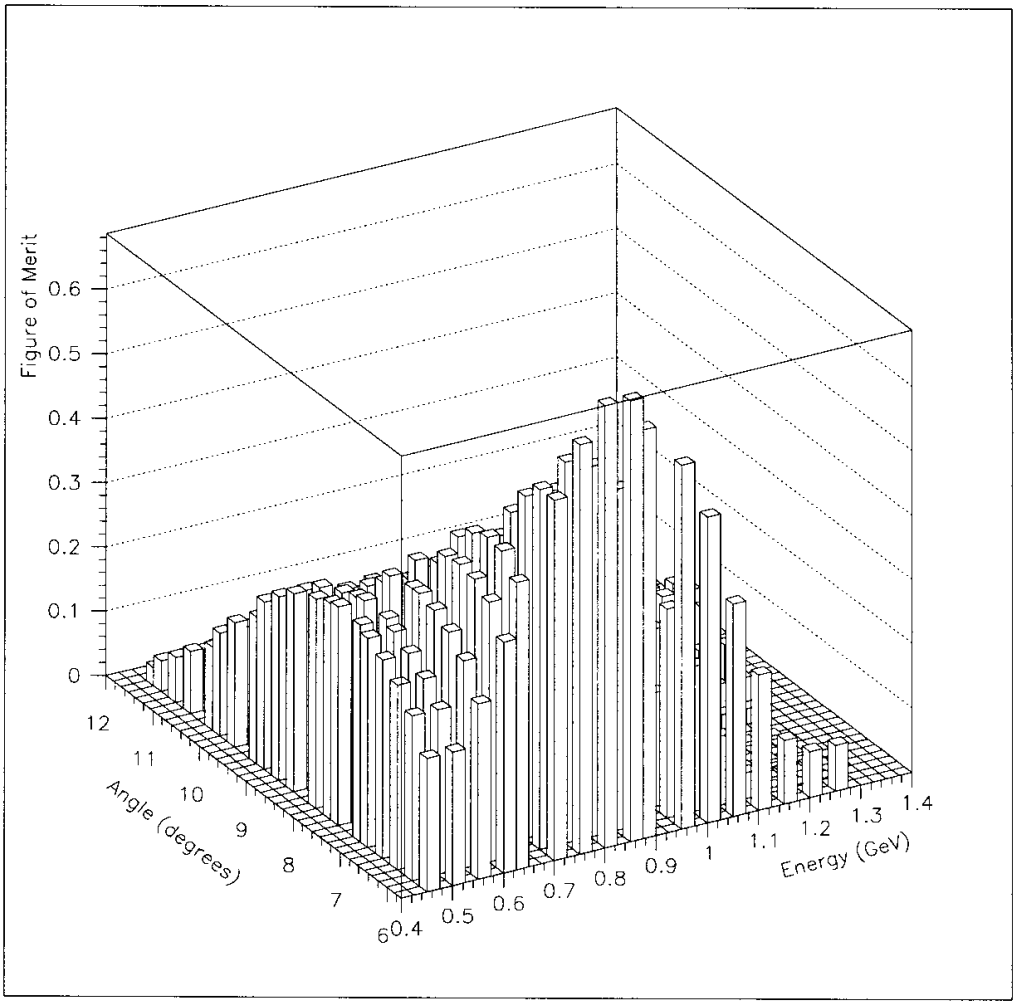

FIGURE 3. Figure of Merit versus Energy and Angle for ^{208}Pb, showing a peak near 850 MeV at an angle of 6 degrees.

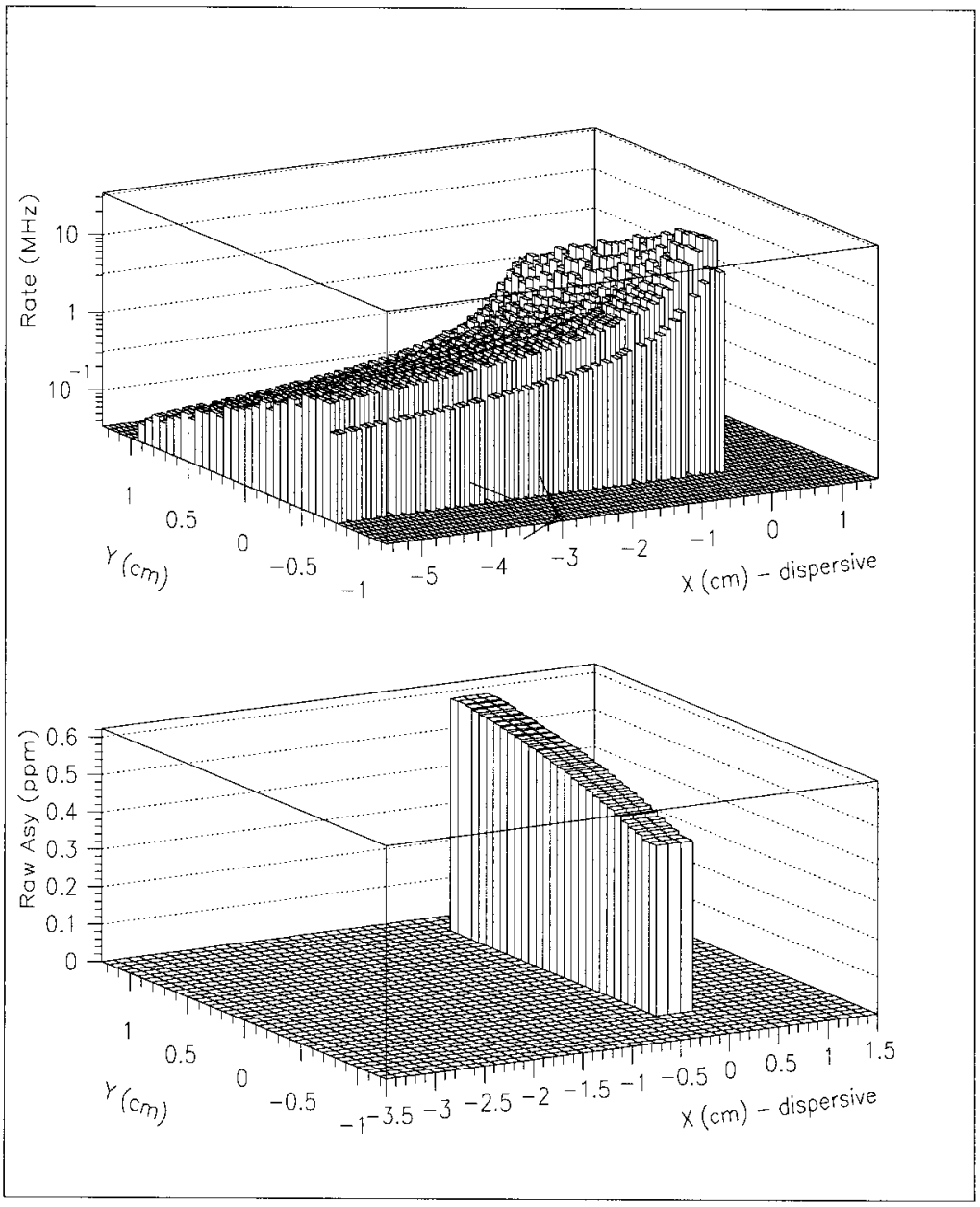

FIGURE 4. The two plots are: a) top: Scattering rate as a function of X-Y position in focal plane. b) bottom: Unradiated raw asymmetry (product of polarization times asymmetry) versus X-Y. Note the different scale in X. The radiative tail, shown in the top figure, extends towards -X. The location of 2 MeV separation from the elastic peak is shown by the arrow at -3 cm in the top figure.

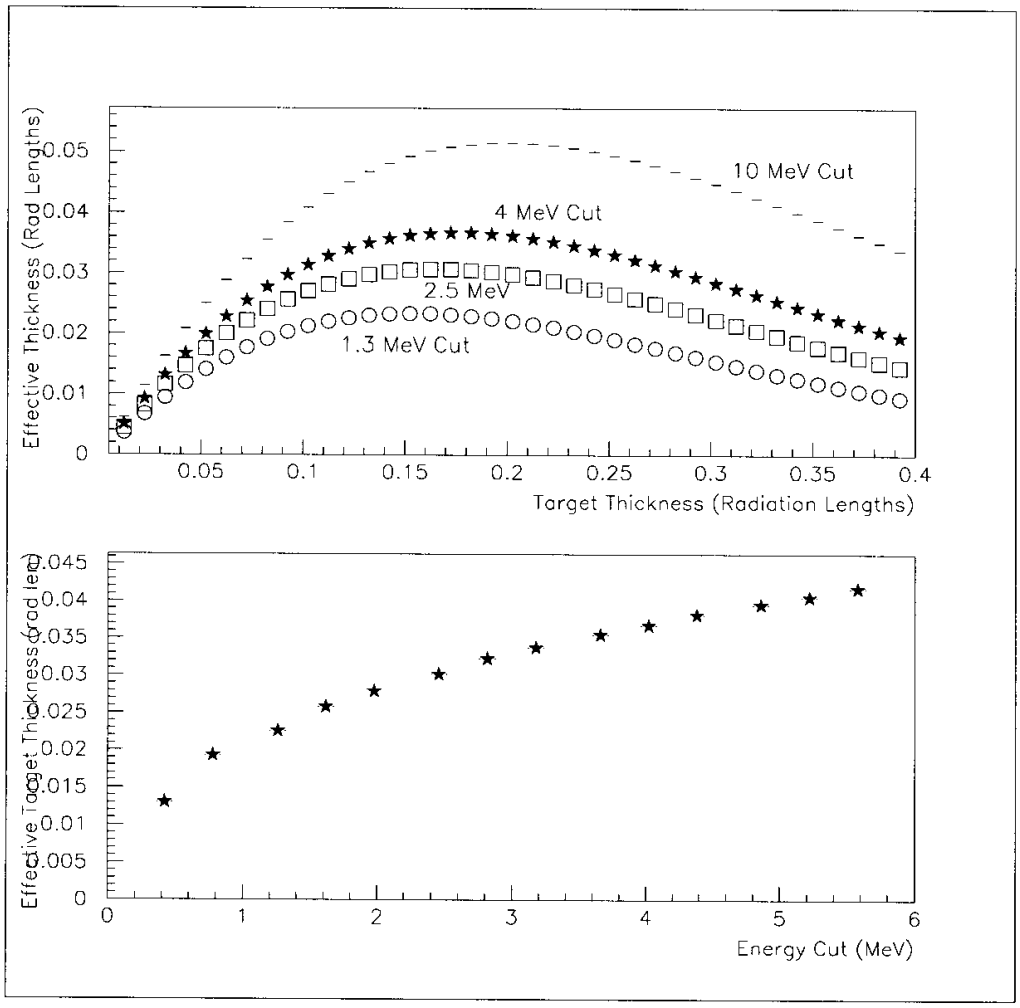

FIGURE 5. Effective target thickness, defined as the product of the actual target thickness times the fraction of events that go into the detector. Top figure: Effective thickness as a function of the actual thickness for various energy cuts imposed by the detector. Bottom figure: The maximum effective thickness as function of the energy cut.

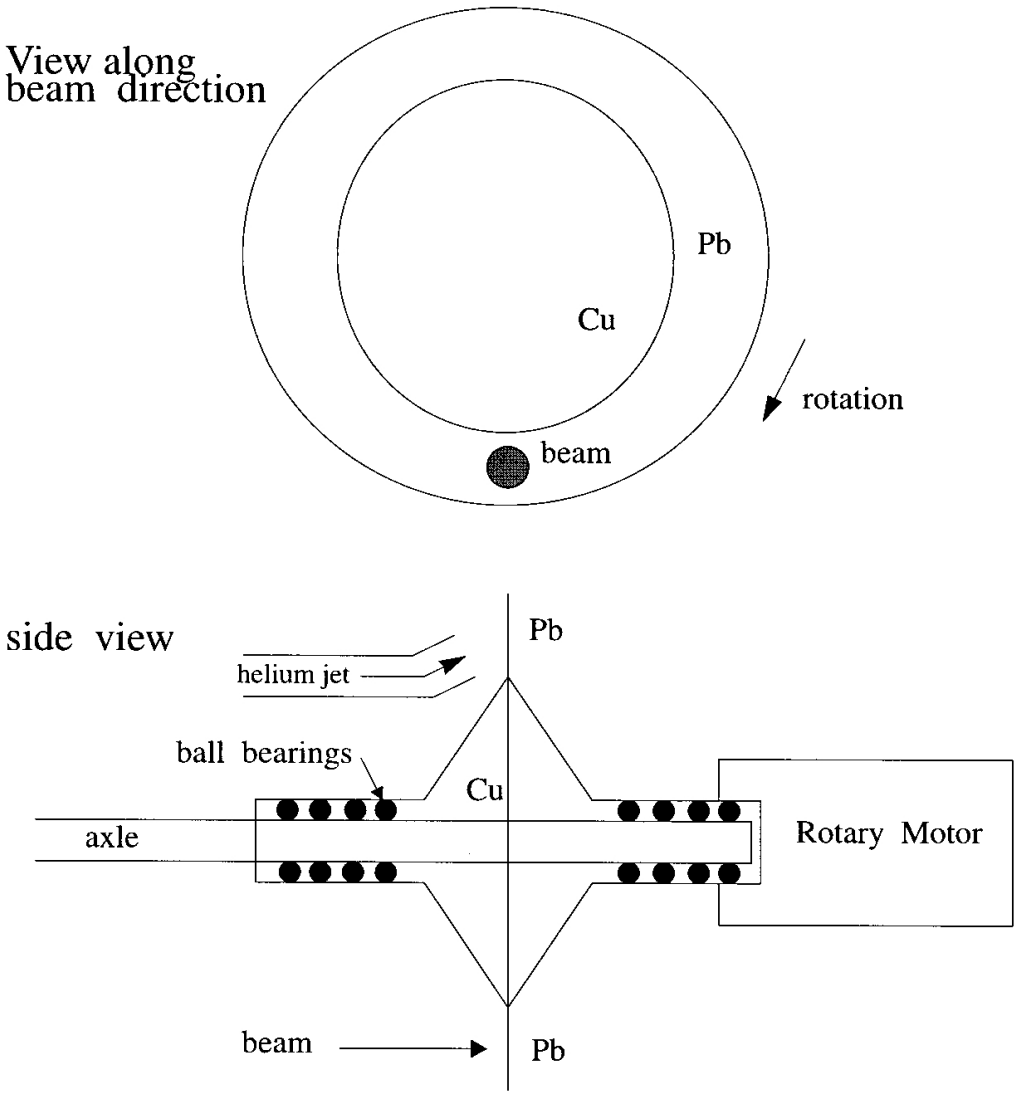

FIGURE 6 Concept of Lead Target. An annulus of lead is attached to a copper wheel which rotates on a water-cooled ball bearing shaft. The beam strikes on the bottom of the orbit, and a possible helium jet is used to cool the top part of the orbit.